Renewable and Sustainable Energy Reviews 151 (2021) 111632

Contents lists available at ScienceDirect

Renewable and Sustainable Energy Reviews

journal homepage: www.elsevier.com/locate/rser

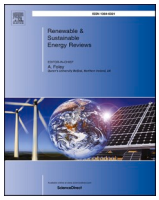

Optimal operation of evaporative cooling pads: A review

A. Tejero-González [a,*], A. Franco-Salas [b]

[a] Department of Energy Engineering and Fluidmechanics, School of Engineering, Universidad de Valladolid, Paseo del Cauce 59, 47011, Valladolid, Spain
[b] ETSIA, University of Sevilla, Ctra. de Utrera Km, 1, 41013, Sevilla, Spain

ARTICLE INFO

Keywords:
Direct evaporative cooling
Evaporative cooling pad
Air conditioning
Cooling efficiency
Saturation effectiveness
Pressure drop

ABSTRACT

Direct evaporative cooling is widely known for being an energy efficient air conditioning solution for arid and/or semi-arid climates. Commercialized evaporative cooling pads vary in material and construction characteristics, while existing research proposes several alternative wetted media and configurations. The most studied factors on the evaporative cooling pads operation are the air velocity or air mass flow rate, air psychrometric conditions; the pad thickness, its geometric characteristics and configuration, and the water flow rate supplied. The pads performance is commonly characterized through its saturation effectiveness, pressure drop, temperature drop and humidity increase achieved in the treated air, water evaporation and consumption, cooling capacity, coefficient of performance and the heat and mass transfer coefficients. Present work conducts a critical review on the existing experimental and theoretical research on commercial and alternative wetted media, identifies the gaps in the literature, proposes uniform nomenclature and methodologies, and provides a critical view on the optimal operating conditions from wetted-surface evaporative coolers.

1. Introduction

Due to nowadays concerns on reducing energy consumption in the building sector, passive cooling techniques are regaining our attention. Among these passive cooling strategies is evaporative cooling [1]. As it spontaneously occurs when water comes into contact with non-saturated air, evaporative cooling is a natural phenomenon and is applied by most animals and plants to control their temperature. Since the ancient civilizations, humankind has used this simple, economic cooling technique to reduce the ambient temperature down to comfort conditions [2].

When evaporatively cooled, humid air has its Dry Bulb Temperature (DBT) decreased close to its wet bulb temperature (WBT) as it gets saturated, due to the heat and mass transfer involved in the phenomenon. To achieve this, evaporative cooling can be implemented either from a humid surface or by spraying water directly in the air. The former option bases on the use of wetted porous media, commonly called "evaporative cooling pads". It is to be noted that performing the evaporative cooling effect from a humid media can enhance the water evaporation rate, hence the cooling effect achieved, compared to directly spraying the water within the airflow [3].

When evaporatively cooled air is directly driven to the occupied spaces, it is called Direct Evaporative Cooling (DEC). DEC systems are widely used in applications such as greenhouses [4], intensive livestock farming [5], industrial facilities [6] and urban outdoor spaces [7,8].

1.1. Wetted porous mediums for evaporative cooling

In evaporative cooling pads, air is usually forced through the media counterflow to water supplied over the media from an upper distributor. The wetted pad then enables the heat and mass transfer between air and water. The ideal characteristics and operation expected in DEC pads are:

- Large, completely wetted water-to-air contact surfaces to achieve maximum air saturation.
- Minimum pressure drop.
- Rigid media that can be easily assembled and dismantled.
- Easy cleaning and maintenance.

Evaporative cooling pads can be classified according to their material and configuration in fiber pads, rigid media pads, and packages or fill pads (Fig. 1).

Fiber pads frequently consist of vegetable fibers, specially aspen [9], but they can also be made of synthetic fibers. Traditional pads are of this type, due to their simplicity; however, they require careful processing and packaging. Current interest on these pads relies on the use of locally available fibers to build cheap and sustainable systems [10].

* Corresponding author.
E-mail address: anatej@eii.uva.es (A. Tejero-González).

https://doi.org/10.1016/j.rser.2021.111632
Received 15 July 2021; Accepted 28 August 2021
Available online 6 September 2021

Abbreviations

COP	Coefficient of Performance
DBT	Dry Bulb Temperature
DEC	Direct Evaporative Cooling
HVAC	Heating, Ventilation and Air Conditioning
IEC	Indirect Evaporative Cooling
WBD	Wet Bulb Depression
WBT	Wet Bulb Temperature

Nomenclature

A	pad contact area (m^2)
As	specific area or pad contact area per unit volume ($m^2 \cdot m^{-3}$)
CC	cooling capacity (W)
Cp	specific heat ($J \cdot kg^{-1} \cdot K^{-1}$)
l	pad thickness (m)
le	pad characteristic length (m)
m	mass flow rate ($kg \cdot s^{-1}$)
RH	Relative Humidity (%)
T	temperature (°C)
v	air velocity ($m \cdot s^{-1}$)
V	evaporative cooling pad volume (m^3)
w	humidity ratio ($kg \cdot kg^{-1}$)
W	power (W)

Subscripts

a	air
ew	evaporated water
f	fan
in	system inlet airflow
out	system outlet airflow
p	pump
w	water
wb	wet bulb

Rigid media pads are made of corrugated plates assembled with resin adhesives to form two different flute angles from the horizontal. Common pad thickness are in the range between 5 and 30 cm. Most rigid media pads are made of cellulose; alternative materials are plastic PVC or polyethylene, glass fiber, carbon fiber, or metallic plates. They enable large water-to-air contact areas, avoid fiber carryout and have longer lifespans than fiber panels [11,12].

Packages or fill pads refer to all porous, inorganic materials either natural, such as volcanic stones [13], or artificial, like expanded clay [14]. As they use less structured materials, they require a case to contain the wetted media and distribute the air and water flows within. Trickle fills are fill pads made of plastic or metal mesh, which present less incrustations and admit larger air and water flows with limited pressure drop and high saturation effectiveness [15,16].

1.2. Justification and objectives

Evaporative cooling from wetted media has been subject of different review articles, generally as part of a wider approach covering different evaporative cooling technologies and sometimes focused on their applicability in buildings, specially intensive farm buildings, and greenhouses [4,6,17–20]. Materials used in direct evaporative cooling systems are also the target of existing review works [21–23].

The present review article focuses on the evaporative cooling from wetted media, though does not aim at simply reviewing the existing materials or configurations. The main objective is to provide insight on the key factors affecting the performance of evaporative cooling wetted media and enhance the scientific impact of future research on the topic, through the following:

1) Serve as reference for all future researchers on DEC media to quickly identify existing literature on the same type of media and parameters they aim to study. This would help researchers to compare their results to existing ones.
2) Develop a critical revision of existing results and determine the optimal operating conditions of different DEC media, identifying the main gaps in the literature to guide and enhance future research conducted towards these issues.
3) Propose a uniform nomenclature and procedures of characterization of DEC media.

Towards these targets, this review article is structured and follows the methodology described in the next section 2.

2. Methodology

A systematic revision of existing research on the behavior of Direct Evaporative Cooling media was conducted, disregarding the application. Databases used for searching the existing literature were Scopus, Web of Science and Google Scholar. Because the present work focuses on the performance of wetted media rather than on their applicability, searches performed were not limited to the recent developments. Articles with limited international impact have been included when approached new materials or configurations.

The present review focuses only on published research meeting the following criteria:

1) It covers all DEC systems based on evaporation from humid surfaces, disregarding the application and including both commercial pads and new prototypes. Consequently, humidification media used in some of the articles reviewed do not correspond to the commonly

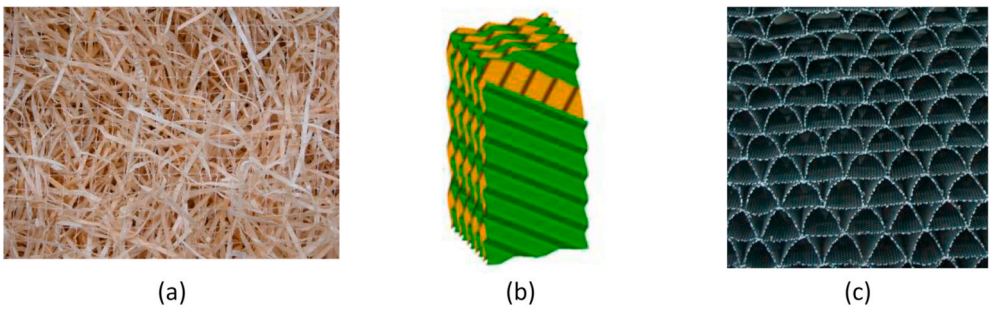

Fig. 1. Example of wetted porous mediums, (a) fiber pads, (b) rigid media pads and (c) packages or fill pads.

called "pad", but to different designs or configurations. Spray systems are excluded.
2) Articles must not necessarily focus on DEC applications, but report data on the behavior of direct humidification media.
3) Porous media operating as what is commonly called "semi-indirect" evaporative cooling are not included, unless they provide insight on the role of the operating factors targeted in the present review.
4) Articles that only reported the comfort conditions achieved at a target space were also excluded, unless the air conditions at the pad inlet and outlet were provided.
5) Results analyzed belong to research works either based on mathematical models or experimental results. Those articles proposing mathematical models that are validated with original experimental results are classified as both "mathematical models" and "experimental research".
6) Due to limitations in its length, the present work only approaches the main performance parameters and influencing factors. Other less studied parameters and factors will be subject to future revision.

Once selected the target works, the performance factors and parameters studied are identified. Special attention is given to those articles proposing optimal operating conditions.

To ease the readers identifying the sort of system they are interested in, reviewed articles are first classified depending on the "types of evaporative cooling pads" (section 3). Then, section 4 "Performance parameters" presents the parameters and factors studied through mathematical models and experimental research. Section 5 "DEC pads operating factors. Optimal performance" develop a comprehensive, critical technical review of the published research, providing global insight on the effect that the main factors studied have on the performance of DEC pads. Results derived from this analysis are then gathered in last section 7 "Conclusions".

For clarity, parameters defined in the references cited are re-expressed here with the nomenclature used in this review work, when possible. Particularly, nomenclature widely varies concerning the most used performance parameter in DEC: the temperature drop achieved to the maximum temperature drop achievable in adiabatic systems, being the latter the difference between the DBT and the WBT of ambient air (or "Wet Bulb Depression" WBD). Indeed, many articles use different terms indistinctively, sometimes when referring to previous results in existing research where a different nomenclature had been used. This lack of a uniform nomenclature may limit the scientific impact of the existing research. Fig. 2 gathers all terms used in the published research reviewed.

Because this parameter expresses a temperature drop, it is commonly called "cooling efficiency/effectiveness"; however, as the psychrometric evolution approaches saturation of air, it is also usually called "saturation efficiency/effectiveness". The terms "efficiency" and "effectiveness" are indeed indistinctively used, sometimes on purpose [17,24,25]. However, the use of the term "efficiency" may be misleading, and "effectiveness" could be more rigorous instead, as no conversion of energy forms is involved in the evaporative cooling phenomenon.

Heating, Ventilation and Air Conditioning (HVAC) handbooks dealing with evaporative cooling systems also use different terms: ASHRAE refers to this parameter either as "Wet Bulb Depression Efficiency" (WBDE) [26] or "direct saturation efficiency" (ε_e) [27]; Wang [28] name it simply "effectiveness", and Watt [2] use the term "saturating efficiency". This incurs in different keywords in the literature for the same concept. It is believed that a uniform nomenclature would enhance the impact of the published research on DEC pads.

Despite widely used, neither "cooling efficiency" or "cooling effectiveness" evidence the different maximum temperature drop achievable in adiabatic systems and one stage Indirect Evaporative Cooling (IEC) systems compared to dew-point Indirect Evaporative Cooling equipment. Indeed, it is often simply referred to as the system (cooler, pad …) "efficiency" or "effectiveness". Khosravi et al. [29] avoid misunderstanding by using the term "cooling effectiveness" to refer to the performance of either adiabatic or dew point evaporative cooling systems, specifying it as "wet-bulb effectiveness" for the former and "dew-point effectiveness" for the latter. Al-Mogbel et al. [30] distinguish "Effectiveness of DEC cooler" from "Effectiveness of IEC cooler". Some authors [10,31–36] define the "cooling efficiency" clarifying that it is the saturation efficiency/effectiveness. Al-Badri and Al-Waaly [37] specify that "the effectiveness of DEC was expressed by the saturation efficiency".

Given the previous reasoning, the authors recommend the use of "saturation effectiveness" because of its rigorousness and given its wide

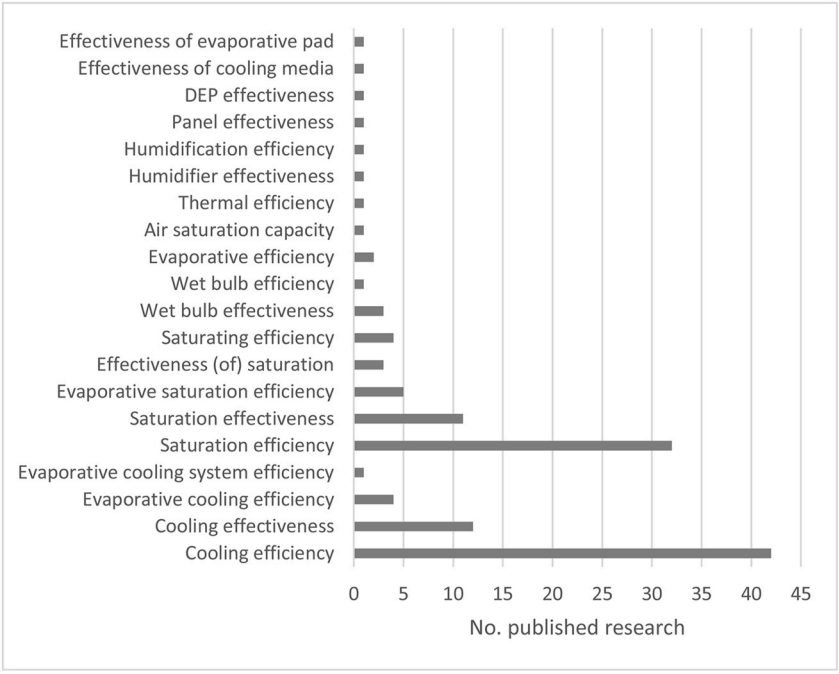

Fig. 2. Nomenclature used in published research for the parameter "saturation effectiveness".

usage.

3. Types of evaporative cooling pads

This section will enable the reader to identify the type of wetted porous medium (or evaporative cooling pad) studied in the research works reviewed.

Among the type of evaporative cooling pads classified in the introduction, rigid media pads studied in the literature are gathered in Table 1, while Table 2 presents the fiber and fill pads. Pad description provided is limited to the information given in the referenced work.

4. Performance parameters

The most studied performance parameters of DEC pads are the saturation effectiveness, pressure drop, humidity increase, water evaporation, temperature drop, cooling capacity, Coefficient of Performance (COP), and the heat and mass transfer coefficients.

As introduced in section 2, the saturation effectiveness relates the temperature drop achieved to the maximum temperature drop achievable in adiabatic systems, which is the difference between the DBT and the WBT of ambient air:

Table 1
Rigid media pad in the literature: materials and geometric characteristics.

Material	Type of pads tested	Geometric characteristics			References
		Angle	Thickness pad	Specific area	
Cellulose	KUUL pad	–	12" (30 cm)	–	[38]
	Kraft and NSSC corrugated	45°–15° with 3 flute sizes: 2.5, 3.5 y 4.5 mm	75 cm	–	[39]
	G&R manufacture	45°–45°	100 mm	391.1 m^2/m^3	[15,40,41]
	Corrugated cellulose by Wadi Group Company	45°–45°	35, 70, 105, and 140 mm	360 m^2/m^3	[31,42]
	Star Cool 7090	45°–45°	100, 150 and 200 mm	–	[43]
	Munters-CELdek 7060-15	45°–15°	100 mm	–	[43,44]
			150, 200 mm	–	[43]
	Munters-CELdek®7060	45°–15°	100, 300 mm	–	[45,46]
	Munters-CELdek®7060	45°–15°	100 mm + 100 mm gap + 100 mm	–	[46]
	Munters-CELdek7060	45°–15°	100, 200 and 300 mm	364.7 m^2/m^3	[47,48]
	Munters-CELdek Cellulose 7060	–	300 mm	–	[49]
	Munters-CELdek	45°–45°	100 mm	347.1 m^2/m^3	[15,40,41]
	Munters-CELdek	60°–30°	50 mm	556.75 m^2/m^3	[15,40,41]
	Munters-CELdek	60°–30°	100 mm	361.5 m^2/m^3	[15,40,41,50]
	Munters-CELdek	60°–30°	50 mm	–	[13,51]
	Munters-CELdek	60°–30°	100 and 150 mm	–	[13]
	Munters-CELdek® 7090–15	60°–30°	100, 150 and 200 mm	–	[43,52]
	Munters-CELdek® 7090–15	–	300 mm	–	[52]
	Munters-CELdek®7090	135°–45°	75, 100, 150 mm	–	[53]
	Munters-CELdek 7090	45° groove angle	100 mm	632 m^2/m^3	[54]
	Munters-CELdek®5090	135°–45°	75, 100, 150 mm	–	[53]
	Munters-CELdek®5090	Varied from 45° to 60° and from 15° to 45°, respectively	Studied in the range from 0.05 to 0.3 m	Studied in the range from 320 to 530 m^2/m^3	[55]
	Rigid cellulose	–	0.15 m	370 m^2/m^3	[56]
	Corrugated paper	–	0.15 m	400 m^2/m^3	[56]
	Corrugated cellulose (not specified)	45°–15°	100, 200 and 300 mm	636 m^2/m^3	[48]
			100, 150, 200 mm	–	[57]
			300 mm	–	[58]
		45°–45°	10 cm	–	[59]
		–	5 cm	100 m^2/m^3	[60]
		–	152 mm	370 m^2/m^3	[61]
		–	3 cm	–	[37]
		–	7.5 cm	–	[62]
		–	42 mm	–	[63]
		–	100 mm	–	[3]
		–	150 mm	–	[64]
		–	0.15 m	–	[65]
		–	–	–	[66,67]
Mixed media	Mixed: corrugated cellulose (CC) and Aspen Fiber (AF)	–	Three thicknesses are used: a) 1 cm AF+2 cm CC b) Two CC layers (4 cm) c) Two AF Layers (2 cm)	–	[30]
Plastic coated cellulose	Plastic coated cellulose rigid cooling pad	45°–15°	138 mm	–	[36]
Glass-Fiber	Munters- GLASdek	Wave angle 90°	138 mm	–	[34,35]
	Glass-Fiber pad	45°–15°	300 mm	–	[58]
PVC	PCV Corrugated media	30°–30°, respectively	100, 200 and 300 mm	211.9 m^2/m^3 respectively	[48]
	PVC 1200	–	300 mm	–	[49]
Trickle	Trickle100 and Trickle125	–	300 mm	–	[49]
Metallic	0.3 mm thick galvanized sheets	Vertical alignment of the sheets with 7.5 mm gap	0.15, 0.30 y 0.45 m	–	[68]
	0.7 mm thick aluminium sheets	The air flows between layers that consist of 2.00 mm longitudinal fins (No. of fins in the air stream is 45)	90 mm	549 m^2/m^3	[69]

Table 2
Fiber and alternative packages pads in the literature: materials and geometric characteristics.

Type of fiber/fill	Material	Geometric characteristics	Thickness pad	References
Vegetable fibers	Aspen	Cooling pads of two different configurations called as Type 1 (25 g fibers) and Type 2 (50 g fibers) distributed inside wire mess frame of size 17 cm × 17 cm	60 cm	[24,70]
		–	7.5 cm	[62]
		Aspen swamp pad	2.5 cm	[59]
		Aspen wood pad, 85 × 73 × 73 cm^3	4 cm	[71]
		Configurations: rectangular, cylindrical, and hexagonal pad. Contact area: 503.6 m^2/m^3	0.15 m	[56]
		Configurations: Three side, triangle, square, pentagon, hexagon, octagon pad. Contact area: 503.7 m^2/m^3	0.15 m	[72]
	Jute	Length/Diameter of fiber: 900/0.1 mm	5 cm	[73]
		Packing density: 20–22 kg/m^3	30 mm	[74]
		Packing density: 62.75 kg/m^3	50, 75 and 100 mm	[25]
	Eucalypt	Density: 495 kg/m^3; Water absorption capacity: 4.3 g/g; Thermal Conductivity: 0.0368–0.0374 W/(m·°C)	65 mm	[29]
		–	–	[10,75]
	Coconut	Coir fiber material pad with a wetted surface area of 250 m^2/m^3	5, 10, and 15 cm	[76]
		Coconut fiber sheets 2 cm thick, forming an angle of 6° at 2 and 10 cm wide.	7 cm	[77]
		Cooling pads of two different configurations called as Type 1 (25 g fibers) and Type 2 (50 g fibers) distributed inside wire mess frame of size 17 cm × 17 cm	60 cm	[24,70]
		Semi-circular, 68.5 cm diameter pad, 83 cm height.		[78]
		Packing density: 25.14 kg/m^3	50, 75 and 100 mm	[25]
		Arranged in a 100 mm × 100 mm x 100 mm frame with mesh. Packing density: 200 kg/m^3	100 mm	[54]
	Palm	Length/Diameter of fiber: 255/0.52 mm	5 cm	[73]
		Packing density: 20–22 kg/m^3	30 mm	[74]
	Luffa	380/0.83 (mm)	5 cm	[73]
		Loofah sponge (Luffa cylindrica) with an average density equal to 19.12 ± 0.89 kg/m^3	5, 7.5, 10 and 12.5 cm	[79]
	Palash fibers and Khus roots	Cooling pads of two different configurations called as Type 1 (25 g fibers) and Type 2 (50 g fibers) distributed inside wire mess frame of size 17 cm × 17 cm	60 cm	[24,70]
	Khus	Semi-circular, 68.5 cm diameter pad, 83 cm height.	–	[78]
	Straw	Straw fiber contained in plastic nets	10 cm	[11]
	Rice husk pads	Local rice husk with average width of 2.02 ± 0.69 mm and length of 10 ± 0.23 Mm	25.4 and 50.8 mm	[80]
Textile fibers and woven fabrics	Nonwoven fabric	A pad made of nonwoven fabric with pin-hole-sized holes (perforated pad in 5 mm diameter of pin- hole and total pin-hole area is about 1/4 of the cross-sectional area of test pad). Wetted surface area: 130 m^2/m^3	5, 10, and 15 cm	[76]
	Curtain fabric and raw cotton fabric	–	–	[81]
	100% cotton fiber	Weight 25 g/m^2	0.1 mm sheets	[82]
	Cotton fabric	25 × 1600 cm^2 piece of cotton fabric, arranged on a wire structure	25 cm	[83]
	Sack cloth	Packing density: 36.62 kg/m^3	50, 75 and 100 mm	[25]
	Synthetic fibers	Synthetic surfactant non-woven and mixed Synthetic/Natural (50% cotton fiber, 30% viscose, 20% polyester). Weight: 50 g/m^2	0.2 mm sheets	[82]
Paper	Kraft paper	Resin treated Kraft paper, Rigid Kraft Paper and Original Kraft paper. Weight 75–125 g/m^2	0.1 mm sheets	[82]
Wood fibers	Bamboo	Semi-circular, 68.5 cm diameter pad, 83 cm height.	–	[78]
	Wood chips	Sliced wood contained in wire nets	10–15 cm	[11]
		Density: 380 kg/m^3; Water absorption capacity: 1.3–1.5 g/g; Thermal Conductivity: 0.08–0.014 W/(m·°C)	65 mm	[29]
	Wood shaving	Arranged in a 100 mm × 100 mm x 100 mm frame with mesh. Packing density: 200 kg/m^3	100 mm	[54]s
Plastic	PVC sponge mesh	Coarse fabric PVC sponge mesh2.5 mm diameter in pinhole and fine fabric PVC sponge mesh in 7.5 mm diameter pinhole	5, 10 and 15 cm	[33]
	Plastic mesh	High density polyethylene folded by means of thermal welding to form triangular flutes arranged vertically. Specific contact surface: 51.77 m^2/m^3 and porosity: 0.969 m^3/m^3	250 mm	[15]
		Cylindrical recycled High-Density Polyethylene (HDPE). Diameter of 3.29 ± 0.62 mm and length of 4.13 ± 0.33 mm	25.4 and 50.8 mm	[80]
		The pad type used is a C&V RF-200 pad with dimensions of 492 × 712 mm. Grid or mesh made with polyethylene yarn, which is 0.7 mm in diameter; 4 × 4 mm ribs are made by thermofusing the material. Pad with a compactness of 117.2 m^2/m^3	80, 160 and 240 mm	[84]
	Shading net	Sun shading ratio of shading net is 0.50	50, 100 and 150 mm	[13]
	High density polythene packing	Wetted surface area: 420 m^2/m^3	0.15 m	[56]
	Polymer hollow fiber	5 fiber bundles (100 fibers each). Tunnel cross section diameter 0.15 m. Packing density 10.67 m^2/m^3	–	[85,86]
Stone	Yellow Stone,	Density: 2880 kg/m^3; Water absorption capacity: 0.024–0.0916 g/g; Thermal Conductivity: 0.6–2.5 W/(m·°C)	65 mm	[29]
		Piece with holes drilled	–	[10]
	Pumice		65 mm	[29]

(*continued on next page*)

Table 2 (*continued*)

Type of fiber/fill	Material	Geometric characteristics	Thickness pad	References
		Density: 250 kg/m^3; Water absorption capacity: 0.024–0.0916 g/g; Thermal Conductivity: 0.186–0.433 W/(m·°C)		
		Pumice stones coarse and fine. Particle size: 20–40 and 10–30 respectively. Dry density: 340–360 kg/m^3	50, 100 and 150 mm	[13]
	Vermiculite	Density: 172 kg/m^3; Water absorption capacity: 3.5–5.9 g/g; Thermal Conductivity: 0.104–0.153 W/(m·°C)	65 mm	[29]
	Vermiculite	Porous pads made from expanded clay (Cinasita). Two granulometries equivalent to Brita 1 and Brita 2	60, 85 or 100 mm	[14]
	Volcanic tuff	Particle size: 15–25. Dry density: 295 kg/m^3	50, 100 and 150 mm	[13]
	Cyprus marble	Cut into shapes to fit in the tunnel	–	[10]
Ceramics	Porous ceramics tubes	Matrix of Porous ceramic pipes arranged vertically with a height of 1200 mm and spaced 58 mm. Outer and inner diameter: 48 and 28 mm, respectively.	600 mm	[87,88]
		Matrix of ceramic tubes consists of 39 ceramic tubes. Material: membrane element made of Al2O3, 1/6 monochannel- design, 0.2 μm pore diameter, 300 mm length. The outer and inner diameter: 10 - 6 mm respectively.	28 cm	[89]
		Matrix of Porous ceramic pipes arranged vertically with a height of 25 cm and spaced 13.5 cm. Outer and inner diameter: 7 and 2.8 cm, respectively. Pore diameter: 5–60 μm, the pore volume:20–40%, the density in completely dry condition: 1300 kg/m^3	3 tubes in staggered-array and parallel arrangement	[90]
	Porous ceramic cylinders	25 cm long, 2 cm diameter tubular rods	–	[91]
		–	–	[10]
	Porous ceramic evaporator prototype	315 mm × 165 mm x 35 mm Low and medium porosity	–	[92]
	Porous ceramic plates	Vertical channel that consisted of two parallel walls separated by a distance 10 cm, on which the external left wall is covered by a ceramic porous layer of different thicknesses (1, 4, 8, 10 mm), and porosities (0.38 and 0.5)	–	[93]
Mixed	Ceramic plates covered with jute fiber	15 plates arranged in five columns, separated 4.6 cm. Total clay surface area 504 cm^2 and jute fiber area 516 cm^2.	–	[94]
Metallic	Copper metal foam pad	Average porosity: 0.82	3 cm	[62]
Others	Dry bulrush basket	–	–	[10]
	Laterite, Fine sand, cement and rice byproducts water-permeable material	600 mm length tubes. Outer and inner diameter: 50.8 and 25.4 mm, respectively. 100 mm × 125 mm x 250 mm blocks.	–	[95]
	Wood charcoal	Packing density: 20–22 kg/m^3	30 mm	[74]
		Pine charcoal with equivalent diameters 30 mm and 50 mm. Each size fraction of the charcoal material was filled separately into galvanized steel frames	100, 200 and 300 mm	[96]

$$\varepsilon = \frac{T_{in} - T_{out}}{T_{in} - T_{wb\ in}} \tag{1}$$

Air humidity increase through the pad is usually studied in terms of the humidity ratio:

$$\Delta w = w_{out} - w_{in} \tag{2}$$

Though sometimes authors simply compare the air relative humidity at the pad outlet to the air conditions at the pad inlet. If the previous equation (2) is multiplied to the air mass flow, it is usually referred as the water evaporation rate:

$$\dot{m}_{ew} = \dot{m}_a \cdot (w_{out} - w_{in}) \tag{3}$$

The term "specific water consumption" is sometimes used to refer to the rate of evaporated water related to the pad frontal area [40,42,55] or the pad volume [55], and the temperature drop achieved [40,42].

The cooling capacity multiplies the temperature drop achieved through the pad to the air specific heat Cp_a and the air mass flow:

$$CC = \dot{m}_a \cdot Cp_a \cdot (T_{in} - T_{out}) \tag{4}$$

whereas the Coefficient of Performance for evaporative cooling systems can be defined as the cooling capacity (equation (4)) related to the electric input power due to the pump (Wp) and fan (Wf):

$$COP = \frac{CC}{\dot{W}_p + \dot{W}_f} \tag{5}$$

Finally, the heat and mass transfer coefficients, namely h_c and h_m, depend on numerous factors and thus it is convenient to work with empirical correlations of dimensionless numbers. Existing research propose different correlations to evaluate their results.

These parameters are gathered in Table 3, related to the influencing factors studied: air velocity (v) or air flow rate ($\dot{m}_a$), air DBT, air humidity (WBT or RH), the pad thickness (l), the pad material, its configuration or other geometric characteristics and the water flow rate ($\dot{m}_w$). Literature is separated in experimental studies and those based on theoretical models. It includes all works giving results on the relation between parameters and factors, even though they do not always provide a detailed discussion. Despite approached in a few works, the air DBT and humidity have no effect on the pressure drop, which is indeed demonstrated by the results shown in these works cited.

5. DEC pads operating factors. Optimal performance

Results obtained in the literature for these operating factors are reviewed and discussed next to provide insight on the optimal performance of DEC from wetted surface.

5.1. Inlet air psychrometric conditions

Most works gathered in Table 3 as providing the operating hygrothermal air conditions (DBT and WBT or RH) do not actually control these factors, and simply measure their variation with time [30,38,51,58–61,63,64,68,73,87–91,94]. Indeed, only a few deliberate on their effect on the DEC behavior.

It is generally accepted that hot, dry conditions are more favorable to the operation of DEC systems [94], while they are put into question for humid climates and for locations where water is scarce [88]. In more humid locations, combination with desiccation [29] or Indirect Evaporative Cooling (IEC) [97] are preferable solutions.

Despite the key effect of air hygrothermal properties on the water evaporation and hence on the performance of the system, perhaps above the remaining factors [98], only a few works in the existing literature

actually control both temperature and relative humidity in their experiments. Experimental results from Camargo et al. [61] show that the saturation effectiveness improves for higher DBT, when "more cooling is necessary to propitiate thermal comfort"; however, no information is given about the air humidity. Similarly, Nada et al. [31,42] observe that larger inlet DBT result into also larger humidity increase and consequent temperature drop, cooling capacity and coefficient of performance, as well as into an increase in the saturation effectiveness, but do not provide information on the inlet air humidity during the tests. Sheng and Nnanna [63] also provide experimental results of the saturation effectiveness increase with the DBT, though observe the relevance of air humidity and propose the study of the saturation effectiveness variation in terms of the "humidity ratio increase" (in g/kg). Chen et al. [85,86] obtain larger temperature drops, as relative humidity decreases, for a given DBT. He et al. [48] refer to the WBD for its significance to the evaporative cooling, but do not control it in their experiments. Velasco-Gómez et al. [83] demonstrate that larger WBD yield larger humidity increase of treated air. As an alternative to the RH or the WBD, Ibrahim et al. [92] resort to the "ambient to saturated vapor pressure difference" to define the force that drives water evaporation from the wetted media.

Simulation studies usually investigate further the effect of hygrothermal conditions. Results from mathematical models agree in that the hygrothermal conditions are determinant for the water evaporation rate. Kovačević and Sourbron [69] observe an increase in the water evaporation rate with larger inlet DBT, and He et al. [50] notice the same effect also for lower relative humidity. Consequently, Sohani et al. [55] notice that water consumption can be excessive for extremely dry conditions of up to 10–20% relative humidity. Larger humidity increase is at the same time evidence of larger temperature drops; in this sense, Sellami et al. [99] found that the outlet temperature was lower as the inlet relative humidity increased. Gilani and Poshtiri [100] indicate that smaller spacing among plates is needed as the air relative humidity increases, then provide a guide for the design of this plate spacing depending on the air conditions. However, despite the effect of the inlet air psychrometric conditions on the temperature and humidity variation, simulation results show a negligible effect on the saturation effectiveness [69,99]. In the same line, Wu et al. [35] notice no effect of the DBT or the WBT on the saturation effectiveness, for air velocities (v) of 2 m/s and pad thickness (l) of 138 mm. Beshkani and Hosseini [57] analyze the effect of the air Prandtl number, which will vary with the DBT, on the saturation effectiveness. They conclude that, for a same Reynolds number, an increase in the Prandtl number from 0.7 to 0.8 yields a 10% decrease in the saturation effectiveness; however, decreasing the Prandtl number to 0.6 shows no effect.

According to the previous results, existing research coincide in the effect of higher DBT and lower RH on the increase of the air humidification, hence the temperature drop, which can be explained on the fundamentals of evaporative cooling. However, some experimental studies observe certain effect of the air DBT on the saturation effectiveness, while in the simulations it appears to be negligible. Larger air humidification evidences an also larger evaporation rate. If this evaporation rate incurs into insufficient wetting of the media due to low water flow rates, then saturation effectiveness will decrease. This will be approached in detain in section 5.5 "water flow rate". If, on contrary, the pad stays completely wetted, inlet air hygrothermal conditions would have no effect on the saturation effectiveness. An increment in the DBT, provided a constant air humidity ratio, yields an also larger difference between this DBT and the ideally achievable WBT (namely, the WBD); as both the actual temperature drop and the maximum one increase, then the saturation effectiveness maintains. The fact that some experimental results show correlation between the DBT and the saturation effectiveness is due to limitations in the approach of the inlet air humidity (provided total wetting of the pad). The effect of air humidity is thus determinant and needs to be carefully approached, preferably controlled, in future experimental research. The DBT should never be studied separately; actually, the WBD arises as a more appropriate parameter to analyze the effect of the air hygrothermal conditions.

Finally, only a few studies determine a range of air psychrometric conditions for which DEC would be practical. Gilani and Poshtiri [100] conclude that DEC is appropriate for climates where DBT varies within the range of 27–41 °C and RH from 10 to 60%. He et al. [49] state that it could be counterproductive to use evaporative cooling pads to precool air before natural draft dry cooling towers if outdoor air DBT is below 20 °C, in the case of cellulose pads, and below 24–26 °C for the remaining materials studied. Nada et al. [31] evaluate the DBT in the range 30°C–50 °C and set the optimal operating conditions at 40 °C.

5.2. Air velocity/flow rate

The air face velocity, or simply air velocity, corresponds to the average velocity measured at the pad inlet/outlet. This is the most studied parameter in the literature, though sometimes evaluated in terms of air flow rate.

High air velocities have been repeatedly correlated to lower saturation effectiveness [16,33,40,46,48,53,61,65,69,74–76,94,96], temperature drop [42,75,91] and relative humidity variation [42,53,91], but also to larger pressure drops [15,31,39,41,46,48,96], water consumption [3,15,31,39,40,42,46,75,91], as well as heat and mass transfer coefficients [3,15,61].

However, some results obtained deserve further attention. For instance, Rong et al. [65] notice that the mass transfer coefficient related to the inlet-to-outlet density difference only depends on the air velocity, then advice that a more thorough study would be necessary. On the other hand, results on the effect of the air velocity on the "water consumption" sometimes differ depending on how this parameter is defined, as indicated in previous section 4.

Greater air face velocities are intrinsically related to higher pressure drops. Malli et al. [53] justify the increase in the pressure drop for larger air velocities not only on the higher resistance to the airflow but also to the worse distribution of the flow field at the pad inlet.

Another unarguably point is the effect of the air velocity on the saturation effectiveness, which is in fact defined as the "common point for all direct evaporative cooling pads" by Laknizi et al. [91]. Indeed, it is concluded from the ANOVA developed by De Melo et al. [79] that the air velocity is determinant on the saturation effectiveness. Higher air face velocities reduce the saturation effectiveness due to lower residence times, hence temperature drops. In their model, Fouda and Melikan [36] obtained shorter transient periods when operating with higher air velocities, but resulted into lower steady-state saturation effectiveness. Although Gunhan et al. [13] observe just a slight decrement of the saturation effectiveness with the air velocity, they conduct tests only for 0.6 and 1 m s^{-1}, with their results actually being in concordance with the remaining literature. Nonetheless, some authors observe that this effect was less significant beyond certain operating conditions. Jain and Hindoliya [24] notice that the effect on the saturation effectiveness softens significantly for airflows above 0.22 kg s^{-1}, while Beshkani and Hosseini [57] notice that the effect of the air velocity on the saturation effectiveness fades once the pad thickness exceeds a certain value. Similarly, Martínez et al. [16] observed the stabilization of the saturation effectiveness for air velocities above 1–1.5 m s^{-1} and for thicker pads. For plastic pads, which are usually of larger thickness, Franco et al. [15] obtained more stable values of the saturation effectiveness, slightly increasing as the air velocity increased from 0.25 m s^{-1} to 2 m s^{-1} but decreasing for even larger air velocities.

Existing research also agree in the increase of the Cooling Capacity with greater air velocity [31,42,52,75], which demonstrates that its effect on the increased mass flow rate of treated air is greater than on the decrease of the temperature achievable. For increasing air velocities up to 0.6 m s^{-1}, Doğramaci et al. [75] obtained a sharp increase of the defined "Specific Cooling Capacity", while it stabilized for even larger air velocities. However, Naveenprabhu and Suresh [3] obtain a negligible influence of the air velocity on the Cooling Capacity. On contrary,

Table 3
Main operating factors and parameters of DEC pads.

Parameter	Factor	Associated studies (models)	Associated experimental studies
Saturation effectiveness	Air velocity (v) or air flow rate ($\dot{m}_a$)	[16,34–36,55–57,61,63,69,72,79,85]	[10,13,15,16,24,25,31–33,39,40,42,44–46,48,51,53,54,58,61,63,65,76,77,79–81,83,85,87,88,91,94,96]
	Air DBT	[35,49,55,61,69,85]	[30,31,42,59–61,63,64,68,83,85,86,88,89,94]
	Air humidity (WBT or RH)	[35,55,69,85]	[30,59,60,64,68,83,85,86,88,89,94]
	Pad thickness (l)	[16,34–36,55,57]	[13,15,16,25,31,33,40,42,45,48,53,68,76,80]
	Configuration/other geometric characteristics of the pad	[55–57,72]	[15,30,39,40,46,53,54,70,87,96]
	Pad material	[49,56]	[10,11,13–15,24,25,29,30,33,39,48,54,59,62,70,76–78,80,81,96]
	Waterflow rate ($\dot{m}_w$)	[none]	[13,16,25,31,40,42,45,46,48,58,64,65,96]
Pressure drop	Air velocity (v) or air flow rate ($\dot{m}_a$)	[16,41,50,55,57,85]	[13–16,25,31,33,38–42,45,46,48,51,53,54,58,76,77,80,83,85,89,96]
	Air DBT	[86]	[31,58,85]
	Air humidity (WBT or RH)	[85]	[85]
	Pad thickness (l)	[16,41,55,57]	[13,14,16,31,33,40,41,45,46,48,53,76,80]
	Configuration/other geometric characteristics of the pad	[41,55,57]	[15,39–41,46,53,54,70,96]
	Pad material	[49]	[13–15,25,33,39,48,54,62,70,76,77,80,96]
	Waterflow rate ($\dot{m}_w$)	[41,50]	[13,15,16,31,40,41,45,48,58,89,96]
Humidity increase	Air velocity (v) or air flow rate ($\dot{m}_a$)	[3,55,69,85]	[3,10,13,16,31,38,39,42,53,54,63,74,75,77,81,85,89,91,94]
	Air DBT	[55,59,69,85]	[31,42,59,63,64,77,83,85,89,94]
	Air humidity (WBT or RH)	[55,59,66,69,85,90]	[38,53,58,59,64,69,83,85,89–91,94]
	Pad thickness (l)	[55]	[13,16,31,42,53]
	Configuration/other geometric characteristics of the pad	[55]	[39,53,54]
	Pad material	[none]	[10,13,29,39,54,58,59,77,78,81]
	Waterflow rate ($\dot{m}_w$)	[3]	[3,16,31,42,64,89]
Water evaporation/water consumption	Air velocity (v) or air flow rate ($\dot{m}_a$)	[43,55,85]	[10,15,16,30,31,39,40,42,45,46,48,53,54,75,85,91,96]
	Air DBT	[50,55,66,85]	[30,31,42,51,64,85,87,88]
	Air humidity (WBT or RH)	[50,55,66,85]	[30,51,64,85,87,88]
	Pad thickness (l)	[43,55]	[15,16,31,40,42,45,46,48,53]
	Configuration/other geometric characteristics of the pad	[43,55]	[15,30,39,46,53,54,96]
	Pad material	[none]	[10,15,30,39,40,48,54,62]
	Waterflow rate ($\dot{m}_w$)	[50]	[16,31,42,48,64,96]
Temperature achieved at the pad outlet/temperature drop	Air velocity (v) or air flow rate ($\dot{m}_a$)	[3,36,43,55,85,100]	[3,10,13,16,31,32,38,39,42,44,63,74,76,77,81,85,91,94]
	Air DBT	[34,35,55,59,61,66,85,100]	[29,31,34,35,37,42,59–61,63,64,68,73,76,85,86,89,91,94]
	Air humidity (WBT or RH)	[34,35,55,59,66,100]	[29,34,35,59,60,64,68,73,76,86,89,94]
	Pad thickness (l)	[36,43,55]	[13,16,31,42,68,76]
	Configuration/other geometric characteristics of the pad	[43,55,100]	[39]
	Pad material	[59]	[10,11,13,24,29,39,59,70,73,74,76–78,81]
	Waterflow rate ($\dot{m}_w$)	[3]	[3,16,31,42,64,89]
Cooling capacity	Air velocity (v) or air flow rate ($\dot{m}_a$)	[3,52,56,72]	[3,10,31,42,54,75,91]
	Air DBT	[none]	[29,31,42,59,60,86]
	Air humidity (WBT or RH)	[none]	[29,59,60,86]
	Pad thickness (l)	[52]	[31,42]
	Configuration/other geometric characteristics of the pad	[56,72]	[54]
	Pad material	[56,59]	[10,29,54,59,62]
	Waterflow rate ($\dot{m}_w$)	[3]	[3,31,42,64]
Coefficient of Performance	Air velocity (v) or air flow rate ($\dot{m}_a$)	[43,52]	[10,31,42,54,75,91]
	Air DBT	[52,59]	[31,42,59]
	Air humidity (WBT or RH)	[59]	[59]
	Pad thickness (l)	[43,52]	[31,42]
	Configuration/other geometric characteristics of the pad	[43]	[54]
	Pad material	[none]	[10,54,59]
	Waterflow rate ($\dot{m}_w$)	[none]	[31,42]
Heat and mass transfer coefficients	Air velocity (v) or air flow rate ($\dot{m}_a$)	[3,33,50,72]	[3,15,33,40,65,77,91]
	Air DBT	[50,85]	[42,85,86]
	Air humidity (WBT or RH)	[50,85]	[85,86]
	Pad thickness (l)	[33,72,76]	[15,33,40,42,46–48,76]
	Configuration/other geometric characteristics of the pad	[69,72]	[15,40,46,77]
	Pad material	[none]	[15,77]
	Waterflow rate ($\dot{m}_w$)	[3]	[3,48]

results on the COP do not always converge. Some authors [31,75] obtain better COPs as the air velocity increases; indeed, Nada et al. [42] obtain the maximum COP at air velocity 2.2 m s^{-1}. However, the COP may not be clearly related to the air velocity due to the additional fan needs [91], which can even result into worse COPs [52].

Many works provide recommended values for the air velocity, generally towards a balanced saturation effectiveness face to the pressure drop. Sohani et al. [55] state that an appropriate air velocity is necessary to optimize both water and electric energy consumption. However, these recommendations are as disparate as the pad types studied.

Wu et al. propose 2.5 m s^{-1} as the optimal air face velocity [34], but recommend carefully selecting the air velocity depending on the pad thickness [35]. Similarly, Malli et al. [53] suggest that the optimal operating conditions imply a certain combination of air velocity and pad thickness, and conclude that it must correspond to lower air face velocities through wider pads. They obtain the maximum saturation effectiveness for air velocities 1.8 m s^{-1} and a pad thickness of 150 mm. For a 70 mm cellulose pad, Nada et al. [31] propose an optimal air velocity of 1 m s^{-1}, obtaining 84% saturation effectiveness and 8 Pa pressure drop when operating with inlet air temperatures of 40 °C, water flow rate 0.1667 kg/s and water temperature 25 °C. In the same line, Martínez et al. [16] propose through an exergetic analysis 1.2, 1.1 and 0.9 m s^{-1} as the optimal air velocities for 80, 160 and 250 mm pad thicknesses. They conclude that optimal air velocities stay far from the extreme values.

Other studies identify the optimal air face velocities for diverse alternative pads. Liao and Chiu [33] develop tests on fabric PVC sponge mesh pads for air face velocities in the range from 0.5 to 2 m s^{-1}. They recommend air velocities between 0.75 and 1.5 m s^{-1} in coarse fabric PVC sponge mesh to balance the effect on the saturation effectiveness and the pressure drop, besides avoiding water carryout; however, they identify the range 1–1.5 m s^{-1} as the "normal" air face velocities. For nonwoven fabric and coir fiber wetting media [76], they obtained optimum air velocities between 1 and 2 m s^{-1}. While operating at constant 35–36 °C DBT and 20% RH with an evaporative cooling pad made of eucalyptus fibers, Doğramaci et al. [75] identified the optimal air velocity and air mass flow rate from the cut point between the Cooling Capacity and the Specific Cooling Capacity, being this optimal conditions between 0.6 and 0.9 m s^{-1} or 0.06–0.08 kg s^{-1} in terms of air mass flow rate. Under these operating conditions, COP was 3.65, Cooling Capacity reached 0.44 kW with 0.27 g s^{-1} water evaporation. In a later work on five different pads [10], they identify the optimal airflow as the cut point between the CC and the saturation effectiveness, yielding the value 0.063 kg s^{-1} as the optimal airflow. If the cut point between the COP and the increment in the humidity ratio was considered, optimal airflow was be 0.041 kg s^{-1}. Ndukwu and Manuwa [74] recommend air velocities of 4 m s^{-1} in alternative latex foam, jute fiber, palm fiber and wood charcoal pads. However, tests are conducted only within the range 3–4.51 m s^{-1} and they do not analyze the effect on the pressure drop. Abdullah et al. [94] recommend the lowest air velocities of about 1 m s^{-1} at which they conduct tests on a jute coated ceramic DEC media, but do not optimize this selection on any other basis rather than the maximum saturation effectiveness achievable.

It must be noted that conclusions derived from experimental results only apply to the type of pad studied and should not be conceived as general design recommendations. Franco et al. [40] recommend operating between 1 and 1.5 m s^{-1}, similar to the 1.27 m s^{-1} proposed in the ASABE standard ANSI/ASAE EP406.4 [9] for 100 mm thick cellulose pads, whereas a 25% lower air face velocity would be acceptable for 50 mm pads. Saturation effectiveness at these air velocities vary from 64% to 70%, pressure drop reaches 3.9–11.25 Pa and water evaporation are within the range 1.8–2.62 kg s^{-1} $m^{-2}{\cdot}K^{-1}$.

5.3. Pad geometric characteristics and configuration

The most studied geometric characteristic is the pad thickness (l), which corresponds to the distance traversed by the airflow. Contact area between water, hence the heat and mass transfer, increases in evaporative cooling pads characterized by larger thicknesses due to larger residence times. Consequently, existing research agree in the fact that an increase in the pad thickness results into larger saturation effectiveness, water evaporation rate and temperature drop [15,35,36,39,48,53,55,99]. Beshkani and Hosseini [57] observe that the saturation effectiveness increases with the pad thickness while Re decreases, and obtain the best result for d = 30 cm and Re = 300. Moreover, as seen in the previous section 5.2, the saturation effectiveness gets almost independent from the air velocity as the pad thicknesses increases [57].

According to the definition of the cooling capacity (equation (4)), larger pad thickness would also result into better cooling capacity, as observed by Nada et al. [42]. Similar results were obtained for fiber pads [13,25] and fill pads like PVC sponge [76], high-density polyethylene mesh [16], or clay [14].

However, results do not agree in terms of the COP; while in their experiments Nada et al. [31,42] obtain better COPs for larger pad thicknesses, Laknizi et al. [52] observe through simulation that the pad thickness would reduce the value of the COP. In fact, the effect of the pad thickness on the COP cannot be generalized because it depends on the power requirements of the fan (equation (5)); larger thicknesses introduce further pressure drop, hence fan power needs, that may or not be compensated by the larger pressure drop and consequent cooling capacity. In terms of exergy efficiency, Nada et al. [31] obtained slightly better results for a thicker cellulose pad (35 mm–140 mm), whereas for plastic mesh fill pads Martínez et al. [16] observe that the performance decreases for larger thicknesses, varying between around 70% and 94% for 80 mm, 160 mm and 250 mm. Because the pad thickness has two opposite effects on the exergy efficiency (the inlet exergy increases with the water evaporation rate but the exergy destruction is enhanced by the larger heat and mass transfer) [31], these two effects must be carefully studied for each particular case.

On the other hand, it must be noted that larger pad thickness (l) increases the pressure drop, hence the operating costs, as well as the maintenance and investment costs. As it can be deduced from the revision of the literature, the pad thickness must be chosen to find a balance between the saturation effectiveness and the pressure drop. Moreover, larger thicknesses require longer times to reach steady state operation [36].

Among the geometric characteristics of the evaporative cooling pads is also the specific area (A), which is the heat and mass transfer area per unit volume, hence the contact area between water and air (As) related to the pad volume (V):

$$A = A_s/V. \tag{6}$$

The pad thickness and the specific area can be related by a dimensionless geometric parameter (le/l), where the characteristic length of the pad (le) is defined by the relation of the pad volume (V) to the total contact area (As). Given previous equation (6), it would be:

$$\frac{l_e}{l} = \frac{V/A_s}{l} = \frac{V/(A\cdot V)}{l} = \frac{1}{l\cdot A} = l^{-1}\cdot A^{-1} \tag{7}$$

Several research works focused on corrugated rigid media pads correlate this dimensionless parameter (le/l), together with the air and water flow rates, to the evaporative cooling pad performance in terms of saturation effectiveness, pressure drop and heat and mass transfer coefficients [15,16,33,37,42,46,48,55].

Sohani et al. [55] observed that, as the specific area (A) increases, the pressure drop also softly increases, though it soars for specific contact areas above 450 m^2 m^{-3}. They found that the optimal pad thickness (l) and specific area (A) where 70 mm and 420 m^2 m^{-3}, respectively. Other

authors also propose optimal pad thicknesses for their particular case. Dai and Sumathy [67] conclude, through a mathematical model, that the optimal pad thickness would be between 50 and 100 mm. Nada et al. [42] obtain optimal water evaporation rate and saturation effectiveness for the maximum thickness studied, 140 mm.

Other researchers have focused their study on the flute size and angles. Smaller distances between adjacent layers increase the pressure drop, but also the contact area and thus the saturation effectiveness.

Franco et al. [40] characterized the performance of four commercial corrugated cellulose pads from two manufacturers with different flute angles and pad thickness, and analyzed the number and thickness of the sheets, flute length and thickness, specific area, the dimensionless parameter le/l and the dry porosity. They concluded that the water evaporated rate was only slightly affected by the pad type, being mainly influenced by the air velocity. Laknizi et al. [43] studied corrugated cellulose pads with three different flute angles, obtaining the best results for the CELdek® 7090–15. Malli et al. [53] study the pressure drop for three thicknesses of two commercial corrugated cellulose pads, whose distance between two adjacent layers was 50 and 70 mm, respectively. Their results showed that thinner plate separation has noticeable effect on the pressure drop for air velocities above 2.3 m s^{-1}.

Barzegar et al. [39] studied three flute sizes of 4.5 mm, 3.5 mm and 2.5 mm each, which resulted in different separations between layers. The corrugated layers were cut in 45° and 15° and bonded alternately, building three cellulose pads of 0.25 m^2 face area and 75 mm thickness of two different cellulose papers. Smaller flute sizes resulted into larger contact area, hence saturation effectiveness. Gilani and Poshtiri [100] also recommend small separations between layers to enhance the cooling effect achieved. Beshkani and Hosseini [57] developed a mathematical model to study the effect of using corrugated paper compared to plate paper. They obtained high velocities of 2.5 m s^{-1}, the use of corrugated instead of flat paper results in a pressure drop increase of 50%, while saturation effectiveness increases by 40%.

Other authors go in depth in the study of the pad configuration, proposing and analyzing different pad shapes [56,72,78] and multiple stage systems of same [46,96] or different materials [30]. Suranjan Salins et al. [54] also compare the pad performance working in counterflow and crossflow configurations, concluding that the generalized, former one provides better performance. However, both configurations provided similar COP under small air flow rates. Finally, Al Khazraji et al. [38] propose the modulation of the pad to enable partial humidification of the media, obtaining a better control of the outlet air temperature and humidity.

5.4. Pad material

The role of the material used as wetted media in the pad performance is due to its porosity and its possibilities to conform a certain configuration that yields the air-water contact area. As seen in the previous section 5.3, the contact area is determinant for the heat and mass transfer. On the other hand, the pad porosity influences the pressure drop (lower porosity is related to higher pressure drops) and the transient times until total humidification of the pad. While rigid media allows an easy calculation of both the porosity and contact area, it is not as easy for most fiber and fill pads. Although different commercial and alternative materials are studied in the literature, either for rigid media, fiber or fill pads, only a few works compare results among different materials.

Cellulose papers are among the most spread wetted media. Barzegar et al. [39] built cellulose corrugated pads with two different type of sheets: Kraft paper and NSSC (Neutral Sulfite Semi Chemical) paper, retaining more water and thus obtaining better saturation effectiveness with the former.

Some alternative materials to cellulose can be attractive in terms of durability, fire resistance, etc. This has led some authors to compare its performance to that of plastic or glass fiber commercial wetted media. He et al. [48] compare cellulose to PVC corrugated pads for air pre-cooling in natural draft dry cooling towers. They obtained better saturation effectiveness in the case of the cellulose material for the same air velocity and pad thickness. These results must nonetheless be considered with care, as the specific area of the cellulose pad was more than 133 m^2 m^{-3} larger than 1.5 times that of the PVC pad. Through a mathematical model developed in a later work [49], they compared four wetted media (cellulose, PVC and two trickle media), obtaining better balanced saturation effectiveness and pressure drops in the cellulose pad. Franco et al. [15] also compare cellulose pads to plastic grid blocks, obtaining larger saturation effectiveness with the plastic grid and remarking the relevance of the pressure drops in the cellulose pads. Cellulose is compared to glass fiber by Sreeram et al. [58]. Under similar operating conditions, glass fiber results into larger pressure drops and slightly lower saturation effectiveness. Given the higher cost of glass fiber pads, their fire resistance is said to be the main advantage. However, the pads studied are insufficiently described to enable a proper comparison of the wetted media performance.

Some authors go beyond the commercialized media and compare the performance of other alternative materials to that of cellulose pads. Rawangkul et al. [77] built two types of coconut coir cooling pads to achieve similar saturation effectiveness than those in a commercial cellulose pad. An appropriate design of the material disposition enabled same similar saturation effectiveness with lower pressure drops. On contrary, Suranjan Salins et al. [54] obtained a much lower saturation effectiveness with coconut coir than with cellulose, proposing wood shaving as a better alternative. Rosa et al. [14] also achieved similar saturation effectiveness to cellulose using expanded clay, observing noticeable deviation in results between different granulometry. Ahmed et al. [11] obtained better saturation effectiveness with sliced wood pads than cellulose, but straw pads had low saturation effectiveness. Gunhan et al. [13] compare CELdek® pads to coarse and fine pumice stones, volcanic tuff and shading net, concluding that the commercial cellulose pad was the best option in terms of pressure drop and saturation effectiveness. Lotfizadeh et al. [62] propose a copper metal foam pad, which introduces less water consumption than aspen fiber fill pads and cellulose pads, but with an average saturation effectiveness. A more detailed description of the system and its performance is needed for a proper interpretation of this result.

Further research examined the performance among different fiber or fill pads. Liao et al. [76] characterize a nonwoven fabric pad and a coir fiber pad, studying different thicknesses. The coir fiber pad introduced larger pressure drop but its saturation effectiveness was remarkably better for small thicknesses. Comparing different alternative vegetable fibers to the commercial aspen fiber pads, Al-Sulaiman [73] concluded that jute and luffa can provided better saturation effectiveness than the commercial aspen fibers, though that of palm fibers was worse, but that lifetime of jute was a drawback. Better saturation effectiveness than jute was obtained for coconut coir by Alam et al. [25], who also characterized sack cloth pads, obtaining in that case the lowest saturation effectiveness. Coconut coir was also studied by Suranjan Salins et al. [54], who compared it to wood shavings; in that case, coconut coir resulted into lower pressure drops but also much lower saturation effectiveness and COP. Ndukwu and Manuwa [74] compare shredded latex foam, jute fiber, palm fruit fiber and wood charcoal to evaluate their economic feasibility for the climate of south-western Nigeria. Doğramaci et al. [10] compared vegetable and porous ceramic and stones. They obtained larger water evaporation rates, hence temperature drop, saturation effectiveness and cooling capacity with eucalyptus fibers, then ceramic pipes, yellow stone, dry bulrush basket and, in the last place, cyprus marble.

In other cases, authors designed and built prototypes based on alternative wetted media, analyzing the effect of modifying any characteristic of the media. Liao and Chiu [33] compared the performance of two PVC sponge mesh with coarse fabric 2.5 mm pinhole diameter and fine fabric 7.5 mm pinhole diameter, respectively. For the same pad

thickness and operating air velocities, the coarse fabric PVC sponge provided larger saturation effectiveness, though less remarkable for larger pad thicknesses studied. The saturation effectiveness for the coarse fabric PVC sponge was also less dependent on the air velocity, but the pressure drop was higher and more air velocity dependent in that case. Ibrahim et al. [92] tested ceramic media of three different porosities, obtaining a cooling effect strongly influenced by the porosity, being negligible in low porosity evaporative cooler.

It must be noted that the performance comparison in alternative media should be approached carefully, as the specific areas of the pads studied should be equivalent.

5.5. Water flow rate

Several authors study the effect of the water flow rate supplied to the wetted media. It must be noted that increasing water supply would raise pumping consumption, though slightly; but, on the other hand, excess wetting permits the system wash particles such as dust and pollen, reduce scale deposition and thus decelerate clogging. Moreover, insufficient water flow rates will not ensure total humidification of the media, with the consequent decrease in the saturation effectiveness, while large water flow rates can imply drop entrainment, specially in pads with low thicknesses operating at high air velocities (though water entrainment can be minimized with a due design of the flute angles in corrugated media or the use of drift eliminators). The literature mainly focuses on the effect of the water flow supplied on the saturation effectiveness and the air pressure drop.

Existing results for different types of pad materials and configurations show that, although an increase in the water flow rate results into higher saturation effectiveness [16,31,42], this effect is weak once the media becomes completely wetted [13,46,48,50,96]. The same happens to the heat and mass transfer coefficients [40]. When water supply is stopped, the mass transfer coefficient keeps on increasing until the pad becomes insufficiently wetted to ensure the maximum saturation effectiveness [65]. Al-Badri and Al-Waaly [37] observe that saturation effectiveness increases for lower ratios air/water mass flow. This is because larger air flows result into also larger evaporation rates that can incur into the incomplete humidification of the pad, thus requiring more water supply to reach the minimum water flow for its total humidification. Consequently, it can be said that all results in the existing literature agree in this issue. Nevertheless, appropriate water flow rates that guarantee total humidification will differ among pad materials and configurations because the evaporation rate is also different for each type of fiber [2]. Moreover, it should be noticed the possible water carryout for larger water flow supply [76].

Concerning pressure drop, experimental research proves that supplying water introduces noticeable, additional resistance to the air flow through conventional cellulose and glass fiber pads compared to the airflow through the dry media [41,46,58,65]. This is due to an increase in the resistance of the pad, hence the static pressure [33]. While water is supplied, increasing water flow rates also result into a slight increment of the air pressure drop through the pad, though less remarkable. In fact, results from Zeitoun et al. [89] show no trend of the pressure drop related to the water velocity at constant air velocities. He et al. [48] observe certain increase in the pressure drop with the water flow rate in pads of d = 300 mm thickness and, to a lesser extent, in pads of d = 200 mm, but no effect was noticed in thinner pads of d = 100 mm. Similarly, Yan et al. [45,46] obtained slightly larger pressure drops as the water flow rate increases for pad thicknesss of 300 mm, while it is negligible for d = 100 mm pads, becoming more noticeable as the air speed increases. For cellulose, 100 mm thick pads, operating at air velocities of 1–1.5 m s^{-1}, Franco et al. [41] observed a maximum increase in the pressure drop between 11.7% and 14.6% when the waterflow rate was duplicated from the recommended values by the ASABE [9]. More remarkable is the effect of water flow rate observed in pads made with alternative, vegetable fibers [25], though it was no contrasted to the effect of the air flow through the same pads. Indeed, for alternative pads made with porous stones [13] and bulk charcoal [96] it has a minor role compared to that of the air flow. Given these results, the effect of water flow on the pressure drop can be disregarded in comparison to that of air flow [40,41] and the pad thickness [48], regardless the type of pad.

In order to reduce the pump and fan requirements without hindering the saturation effectiveness, He et al. [48] propose identifying the precise minimum water flow required to maintain the pad completely wetted, though note that larger water flow rates may be needed to reduce incrustations. Ghoname [64] recommends operating with larger water flow rates to minimize clogging and decelerate the deterioration of the pad performance over time, but obtain optimal results for the lowest water flow studied (4.76 l $min^{-1}·m^{-2}$). Yan et al. [46] conduct tests for the water flow rate recommended by the manufacturer (62 l $min^{-1}·m^{-2}$) and half that rate, concluding that a water flow 10 to 30 times the evaporation rate is recommended to fulfill total wetting and remove debris deposited on the wetted media.

Above results show that the water flow rate has a slight effect on the pressure drop, yet depictable if compared to the influence of the air velocity or the pad thickness. A certain effect is also observed on the saturation effectiveness; however, this trend fades once the water flow rate is enough to ensure the pad to be kept totally humid, when the heat and mass transfer coefficients are optimized. Operation with the minimum water flow that guarantees total humidification of the media, hence the maximum saturation effectiveness, could reduce pumping and, by a smaller amount, fan needs; however, it could incur into large salt depositions, hence shorter lifetime of the humid media. Because, as seen before, the water evaporation rate is intrinsically related to the air psychrometric conditions, the water flow rate can be optimized in terms of the latter. Besides, further study of the pads ageing could enlighten the actual needs for water flow rates and bleed-off necessary to minimize incrustations while optimizing water consumption, power needs and proper performance during the pad lifetime.

6. Conclusions

The present work reviews the main factors studied in the literature to characterize the performance of evaporative cooling wetted media. Insights derived on the optimal operation are:

- Optimization of DEC from wetted surface operation must be directed towards a balanced saturation effectiveness and pressure drop, which will derive from an appropriate combination of the air face velocity and pad thickness for each pad type (material and configuration). Results available in existing research are specific for the pad studied and cannot be extrapolated.
- Although larger thicknesses increase the temperature drop and thus the saturation effectiveness and the cooling capacity, the pressure drop also increases, hence the fan requirements. Consequently, the effect of the pad thickness on the COP cannot be generalized and requires a particular study.
- A large number of research works measure but do not control the air psychrometric conditions at the pad inlet. Sometimes attention is only given to the DBT. Due to their influence in the system performance, both DBT and air humidity must be evaluated. The use of the Wet Bulb Depression parameter is recommended.
- Water flow rates have little effect on the pad saturation effectiveness once the media is completely wetted. Its effect on the air pressure drop through the pad can be neglected in comparison to that of air flow and pad thickness, regardless of the pad type. High water flow rates imply more risk of water carryout, but can reduce salt deposition. It is thus recommendable to optimize the water flow rate towards total humidification of the media, hence in terms of air velocity, psychrometric conditions and pad material, while avoiding excessive salt deposition.

For a proper comparison among different wetted media, a technically sound work must provide detailed description of the geometric characteristics of the pads, namely the specific transfer area ($m^2 \cdot m^{-3}$). Because in fiber pads the specific transfer area cannot be determined, another parameter would be necessary for a proper comparison of results among wetted media.

To enhance the impact of the related published research, care should be taken to use uniform nomenclature. This has special relevance for the saturation effectiveness, which is the main performance parameter studied in direct evaporative cooling. Future work will be needed on the revision of other influencing factors studied in the literature such as water temperature, salinity, and solar radiation, as well as pad operating characteristics like water carryout, material decay, transient operation or supply air quality.

Credit author statement

Ana Tejero-González: Conceptualization, Methodology, Investigation, Data curation, Writing-Original draft. Antonio Franco-Salas: Investigation, Data curation, Writing-Reviewing and Editing.

Declaration of competing interest

The authors declare that they have no known competing financial interests or personal relationships that could have appeared to influence the work reported in this paper.

Acknowledgements and funding

This research was supported by the Education Department of the Regional Government of Castile and Leon and the European Regional Development Fund (ERDF) through the research project: “Análisis de tecnologías energéticamente eficientes para la sostenibilidad de los edificios” [grant number: VA272P18].

References

[1] Oropeza-perez I, Østergaard PA. Active and passive cooling methods for dwellings : a review. Renew Sustain Energy Rev 2018;82:531–44. https://doi.org/10.1016/j.rser.2017.09.059.
[2] Watt JR. Evaporative air conditioning handbook. second ed. Boston, MA: Springer US; 1986. https://doi.org/10.1007/978-1-4613-2259-7.
[3] Naveenprabhu V, Suresh M. Performance enhancement studies on evaporative cooling using volumetric heat and mass transfer coefficients. Numer Heat Tran 2020:1–20. https://doi.org/10.1080/10407782.2020.1793556. 0.
[4] Ghani S, Bakochristou F, ElBialy EMAA, Gamaledin SMA, Rashwan MM, Abdelhalim AM, et al. Design challenges of agricultural greenhouses in hot and arid environments – a review. Eng Agric Environ Food 2019;12:48–70. https://doi.org/10.1016/j.eaef.2018.09.004.
[5] Al Assaad DK, Orabi MS, Ghaddar NK, Ghali KF, Salam DA, Ouahrani D, et al. A sustainable localised air distribution system for enhancing thermal environment and indoor air quality of poultry house for semiarid region. Biosyst Eng 2021;203:70–92. https://doi.org/10.1016/j.biosystemseng.2021.01.002.
[6] Xuan YM, Xiao F, Niu XF, Huang X, Wang SW. Research and application of evaporative cooling in China: a review (I) - Research. Renew Sustain Energy Rev 2012;16:3535–46. https://doi.org/10.1016/j.rser.2012.01.052.
[7] Ulpiani G. Water mist spray for outdoor cooling: a systematic review of technologies, methods and impacts. Appl Energy 2019;254:113647. https://doi.org/10.1016/j.apenergy.2019.113647.
[8] Pérez-Urrestarazu L, Fernández-Cañero R, Franco A, Egea G. Influence of an active living wall on indoor temperature and humidity conditions. Ecol Eng 2016;90:120–4. https://doi.org/10.1016/j.ecoleng.2016.01.050.
[9] American Society of Agricultural, Biological Engineers A. ASABE Standard (ANSI/ASAE EP406.4). Heating, ventilating and cooling greenhouses. 2008.
[10] Doğramacı PA, Aydın D. Comparative experimental investigation of novel organic materials for direct evaporative cooling applications in hot-dry climate. J Build Eng 2020;30. https://doi.org/10.1016/j.jobe.2020.101240.
[11] Ahmed EM, Abaas O, Ahmed M, Ismail MR. Performance evaluation of three different types of local evaporative cooling pads in greenhouses in Sudan. Saudi J Biol Sci 2011;18:45–51. https://doi.org/10.1016/j.sjbs.2010.09.005.
[12] Czarick M, Fairchild B. Plastic less effective than paper evaporative cooling pads! World Poultrymeat 2012;28:26–9.
[13] Gunhan T, Demir V, Yagcioglu AK. Evaluation of the suitability of some local materials as cooling pads. Biosyst Eng 2007;96:369–77. https://doi.org/10.1016/j.biosystemseng.2006.12.001.
[14] Rosa JFV, Tinôco IFF, Fernandes CM, Zolnier S, Bueno MM. Análise da Eficiência de Resfriamento de Painéis Porosos Preenchidos com Argila Expandida em Comparação aos de Celulose Usando Túnel de Vento. Rev Eng Na Agric - REVENG 2011;19:516–23. https://doi.org/10.13083/1414-3984.v19n06a03.
[15] Franco A, Valera DL, Peña A. Energy efficiency in greenhouse evaporative cooling techniques: cooling boxes versus cellulose pads. Energies 2014;7:1427–47. https://doi.org/10.3390/en7031427.
[16] Martínez P, Ruiz J, Martínez PJ, Kaiser AS, Lucas M. Experimental study of the energy and exergy performance of a plastic mesh evaporative pad used in air conditioning applications. Appl Therm Eng 2018;138:675–85. https://doi.org/10.1016/j.applthermaleng.2018.04.065.
[17] Cuce PM, Riffat S. A state of the art review of evaporative cooling systems for building applications. Renew Sustain Energy Rev 2016;54:1240–9. https://doi.org/10.1016/j.rser.2015.10.066.
[18] Emdadi Z, Maleki A, Azizi M, Asim N. Evaporative passive cooling designs for buildings. Strateg Plan Energy Environ ISSN 2019;38:63–80. https://doi.org/10.1080/10485236.2019.12054412.
[19] Misra D, Ghosh S. Evaporative cooling technologies for greenhouses: a comprehensive review. Agric Eng Int CIGR J 2018;20:1–15.
[20] Yang Y, Cui G, Lan CQ. Developments in evaporative cooling and enhanced evaporative cooling - a review. Renew Sustain Energy Rev 2019;113:109230. https://doi.org/10.1016/j.rser.2019.06.037.
[21] Kumar S, Singh J, Siyag J, Rambhatla S. Potential alternative materials used in evaporative coolers for sustainable energy applications: a review. Int J Air-Conditioning Refrig 2020;28:2030006. https://doi.org/10.1142/s2010132520300062.
[22] He S, Gurgenci H, Guan Z, Huang X, Lucas M. A review of wetted media with potential application in the pre-cooling of natural draft dry cooling towers. Renew Sustain Energy Rev 2015;44:407–22. https://doi.org/10.1016/j.rser.2014.12.037.
[23] Emdadi Z, Asim N, Yarmo MA, Shamsudin R, Mohammad M, Sopian K. Green material prospects for passive evaporative cooling systems: Geopolymers. Energies 2016;9. https://doi.org/10.3390/en9080586.
[24] Jain JK, Hindoliya DA. Correlations for saturation efficiency of evaporative cooling pads. J Inst Eng Ser C 2014;95:5–10. https://doi.org/10.1007/s40032-014-0098-0.
[25] Alam MF, Sazidy AS, Kabir A, Mridha G, Litu NA, Rahman MA. An experimental study on the design, performance and suitability of evaporative cooling system using different indigenous materials. AIP Conf Proc 2017:1851. https://doi.org/10.1063/1.4984704.
[26] ASHRAE. Evaporative. Cooling. Atlanta: ASHRAE Handb. - HVAC Appl.; 2019.
[27] ASHRAE. Evaporative air-cooling equipment. ASHRAE Handbook. Atlanta: HVAC Syst. Equipment.; 2020.
[28] Wang S. Handbook of air conditioning and refrigeration. second ed. 2000. Michigan.
[29] Khosravi N, Aydin D, Karim Nejhad M, Dogramaci PA. Comparative performance analysis of direct and desiccant assisted evaporative cooling systems using novel candidate materials. Energy Convers Manag 2020;221:113167. https://doi.org/10.1016/j.enconman.2020.113167.
[30] Al-Mogbel A, Hussain S, Rafique MZ, Almeshaal MA. Experimental investigations of evaporative cooling system for buildings in hot and dry environments. Heat Tran Res 2020;51:825–35.
[31] Nada SA, Fouda A, Mahmoud MA, Elattar HF. Experimental investigation of energy and exergy performance of a direct evaporative cooler using a new pad type. Energy Build 2019;203. https://doi.org/10.1016/j.enbuild.2019.109449.
[32] Abohorlu Doğramacı P, Riffat S, Gan G, Aydın D. Experimental study of the potential of eucalyptus fibres for evaporative cooling. Renew Energy 2019;131:250–60. https://doi.org/10.1016/j.renene.2018.07.005.
[33] Liao CM, Chiu KH. Wind tunnel modeling the system performance of alternative evaporative cooling pads in Taiwan region. Build Environ 2002;37:177–87. https://doi.org/10.1016/S0360-1323(00)00098-6.
[34] Wu JM, Huang X, Zhang H. Theoretical analysis on heat and mass transfer in a direct evaporative cooler. Appl Therm Eng 2009;29:980–4. https://doi.org/10.1016/j.applthermaleng.2008.05.016.
[35] Wu JM, Huang X, Zhang H. Numerical investigation on the heat and mass transfer in a direct evaporative cooler. Appl Therm Eng 2009;29:195–201. https://doi.org/10.1016/j.applthermaleng.2008.02.018.
[36] Fouda A, Melikyan Z. A simplified model for analysis of heat and mass transfer in a direct evaporative cooler. Appl Therm Eng 2011;31:932–6. https://doi.org/10.1016/j.applthermaleng.2010.11.016.
[37] Al-Badri AR, Al-Waaly AAY. The influence of chilled water on the performance of direct evaporative cooling. Energy Build 2017;155:143–50. https://doi.org/10.1016/j.enbuild.2017.09.021.
[38] Al Khazraji A, Siddarth A, Varadharasan M, Guhe A, Agonafer D, Hoverson J, et al. Experimental characterization of vertically split distribution wet- cooling media used in the direct evaporative cooling of data centers. Proc 17th Intersoc Conf Therm Thermomechanical Phenom Electron Syst ITherm 2018 2018. https://doi.org/10.1109/ITHERM.2018.8419611. 971–8.
[39] Barzegar M, Layeghi M, Ebrahimi G, Hamzeh Y, Khorasani M. Experimental evaluation of the performances of cellulosic pads made out of Kraft and NSSC corrugated papers as evaporative media. Energy Convers Manag 2012;54:24–9. https://doi.org/10.1016/j.enconman.2011.09.016.
[40] Franco A, Valera DL, Madueño A, Peña A. Influence OF water and air flow ON the performance OF cellulose evaporative cooling pads used IN mediterranean greenhouses. Trans ASABE (Am Soc Agric Biol Eng) 2010;53:565–76.

[41] Franco A, Valera DL, Peña A, Pérez AM. Aerodynamic analysis and CFD simulation of several cellulose evaporative cooling pads used in Mediterranean greenhouses. Comput Electron Agric 2011;76:218–30. https://doi.org/10.1016/j.compag.2011.01.019.

[42] Nada SA, Elattar HF, Mahoud MA, Fouda A. Performance enhancement and heat and mass transfer characteristics of direct evaporative building free cooling using corrugated cellulose papers. Energy 2020;211. https://doi.org/10.1016/j.energy.2020.118678.

[43] Laknizi A, Abdellah A Ben, Mahdaoui M. Application of Taguchi and ANOVA methods in the optimisation of a direct evaporative cooling pad. Int J Sustain Eng 2021:1–11. https://doi.org/10.1080/19397038.2020.1866707. 00.

[44] Dağtekin M, Karaca C, Yildiz YI, Başçetinçelik A, Ö Paydak. The effects of air velocity on the performance of pad evaporative cooling systems. Afr J Agric Res 2011;6:1813–22. https://doi.org/10.5897/AJAR10.1110.

[45] Yan M, He S, Gao M, Xu M, Miao J, Huang X, et al. Comparative study on the cooling performance of evaporative cooling systems using seawater and freshwater. Int J Refrig 2020. https://doi.org/10.1016/j.ijrefrig.2020.10.003.

[46] Yan M, He S, Li N, Huang X, Gao M, Xu M, et al. Experimental investigation on a novel arrangement of wet medium for evaporative cooling of air. Int J Refrig 2020:1–11. https://doi.org/10.1016/j.ijrefrig.2020.12.014. 0.

[47] He S, Guan Z, Gurgenci H, Hooman K, Alkhedhair AM. Experimental study of heat transfer coefficient and pressure drop of cellulose corrugated media. Proc 19th Australas Fluid Mech Conf AFMC 2014 2014:3–6.

[48] He S, Guan Z, Gurgenci H, Hooman K, Lu Y, Alkhedhair AM. Experimental study of film media used for evaporative pre-cooling of air. Energy Convers Manag 2014;87:874–84. https://doi.org/10.1016/j.enconman.2014.07.084.

[49] He S, Xu Y, Zhang G, Hooman K, Gao M. Selection of wetted media for pre-cooling of air entering natural draft dry cooling towers. Appl Therm Eng 2017;114:857–63. https://doi.org/10.1016/j.applthermaleng.2016.11.179.

[50] He S, Guan Z, Gurgenci H, Jahn I, Lu Y, Alkhedhair A M. Influence of ambient conditions and water flow on the performance of pre-cooled natural draft dry cooling towers. Appl Therm Eng 2014;66:621–31. https://doi.org/10.1016/j.applthermaleng.2014.02.070.

[51] Franco-Salas A, Peña-Fernández A, Valera-Martínez DL. Refrigeration capacity and effect of ageing on the operation of cellulose evaporative cooling pads, by wind tunnel analysis. Int J Environ Res Publ Health 2019;16. https://doi.org/10.3390/ijerph16234690.

[52] Laknizi A, Mahdaoui M, Ben Abdellah A, Anoune K, Bakhouya M, Ezbakhe H. Performance analysis and optimal parameters of a direct evaporative pad cooling system under the climate conditions of Morocco. Case Stud Therm Eng 2019;13:100362. https://doi.org/10.1016/j.csite.2018.11.013.

[53] Malli A, Seyf HR, Layeghi M, Sharifian S, Behravesh H. Investigating the performance of cellulosic evaporative cooling pads. Energy Convers Manag 2011;52:2598–603. https://doi.org/10.1016/j.enconman.2010.12.015.

[54] Suranjan Salins S, Kota Reddy S, Kumar S. Experimental investigation on use of alternative innovative materials for sustainable cooling applications 2021. doi:10.1080/19397038.2021.1924894.

[55] Sohani A, Zabihigivi M, Moradi MH, Sayyaadi H, Hasani Balyani H. A comprehensive performance investigation of cellulose evaporative cooling pad systems using predictive approaches. Appl Therm Eng 2017;110:1589–608. https://doi.org/10.1016/j.applthermaleng.2016.08.216.

[56] Kulkarni RK, Rajput SPS. Comparative performance anlysis of evaporative cooling pads of alternative configurations and materials. Int J Adv Eng 2013;6:1524–34.

[57] Beshkani A, Hosseini R. Numerical modeling of rigid media evaporative cooler. Appl Therm Eng 2006;26:636–43. https://doi.org/10.1016/j.applthermaleng.2005.06.006.

[58] Sreeram V, Gebrehiwot B, Sathyanarayan S, Sawant D, Agonafer D, Kannan N, et al. Factors that affect the performance characteristics of wet cooling pads for data center applications. Annu IEEE Semicond Therm Meas Manag Symp 2015. https://doi.org/10.1109/SEMI-THERM.2015.7100160. 2015-April:195–202.

[59] Bishoyi D, Sudhakar K. Experimental performance of a direct evaporative cooler in composite climate of India. Energy Build 2017;153:190–200. https://doi.org/10.1016/j.enbuild.2017.08.014.

[60] Mohammad AT, Mat S Bin, Sulaiman MY, Sopian K, Al-Abidi AA. Experimental performance of a direct evaporative cooler operating in kuala lumpur. Int J Therm Environ Eng 2013;6:15–20. https://doi.org/10.5383/ijtee.06.01.003.

[61] Camargo JR, Ebinuma CD, Silveira JL. Experimental performance of a direct evaporative cooler operating during summer in a Brazilian city. Int J Refrig 2005;28:1124–32. https://doi.org/10.1016/j.ijrefrig.2004.12.011.

[62] Lotfizadeh H, Razzaghi H, Layeghi M. Experimental performance analysis of a solar evaporative cooler with three different types of pads. J Renew Sustain Energy 2013;5:1–14. https://doi.org/10.1063/1.4831779.

[63] Sheng C, Agwu Nnanna AG. Empirical correlation of cooling efficiency and transport phenomena of direct evaporative cooler. Appl Therm Eng 2012;40:48–55. https://doi.org/10.1016/j.applthermaleng.2012.01.052.

[64] Ghoname MS. Effect of pad water flow rate on evaporative cooling system efficiency in laying hen housing. J Agric Eng 2020;51:209–19. https://doi.org/10.4081/jae.2020.1051.

[65] Rong L, Pedersen P, Jensen TL, Morsing S, Zhang G. Dynamic performance of an evaporative cooling pad investigated in a wind tunnel for application in hot and arid climate. Biosyst Eng 2017;156:173–82. https://doi.org/10.1016/j.biosystemseng.2017.02.003.

[66] Kabeel AE, Bassuoni MM. A simplified experimentally tested theoretical model to reduce water consumption of a direct evaporative cooler for dry climates. Int J Refrig 2017;82:487–94. https://doi.org/10.1016/j.ijrefrig.2017.06.010.

[67] Dai YJ, Sumathy K. Theoretical study on a cross-flow direct evaporative cooler using honeycomb paper as packing material. Appl Therm Eng 2002;22:1417–30. https://doi.org/10.1016/S1359-4311(02)00069-8.

[68] Alodan MA, Al-Faraj AA. Design and evaluation of galvanized metal sheets as evaporative cooling pads. Agric Sci 2005;18:9–18.

[69] Kovačević I, Sourbron M. The numerical model for direct evaporative cooler. Appl Therm Eng 2017;113:8–19. https://doi.org/10.1016/j.applthermaleng.2016.11.025.

[70] Jain JK, Hindoliya DA. Experimental performance of new evaporative cooling pad materials. Sustain Cities Soc 2011;1:252–6. https://doi.org/10.1016/j.scs.2011.07.005.

[71] Alamdari P, Saedodin S, Rejvani M. Do non-metallic material and radiation shields affect the operation of direct evaporative cooling systems? Int J Refrig 2020;114:98–105. https://doi.org/10.1016/j.ijrefrig.2020.02.038.

[72] Dhamneya AK, Rajput SPS, Singh A. Thermodynamic performance analysis of direct evaporative cooling system for increased heat and mass transfer area. Ain Shams Eng J 2018;9:2951–60. https://doi.org/10.1016/j.asej.2017.09.008.

[73] Al-Sulaiman F. Evaluation of the performance of local fibers in evaporative cooling. Energy Convers Manag 2002;43:2267–73. https://doi.org/10.1016/S0196-8904(01)00121-2.

[74] Ndukwu MC, Manuwa SI. A techno-economic assessment for viability of some waste as cooling pads in evaporative cooling system. Int J Agric Biol Eng 2015;8:151–8. https://doi.org/10.3965/j.ijabe.20150802.952.

[75] Doğramacı PA, Riffat S, Gan G, Aydın D. Experimental study of the potential of eucalyptus fibres for evaporative cooling. Renew Energy 2019;131:250–60. https://doi.org/10.1016/j.renene.2018.07.005.

[76] Liao CM, Singh S, Wang T. Sen. Characterizing the performance of alternative evaporative cooling pad media in thermal environmental control applications. J Environ Sci Heal - Part A Toxic/Hazardous Subst Environ Eng 1998;33:1391–417. https://doi.org/10.1080/10934529809376795.

[77] Rawangkul R, Khedari J, Hirunlabh J, Zeghmati B. Performance analysis of a new sustainable evaporative cooling pad made from coconut coir. Int J Sustain Eng 2008;1:117–31. https://doi.org/10.1080/19397030802326726.

[78] Shekhar R, Chopra MK, Purohit R. Design of compact evaporative cooler to improve cooling efficiency and to evaluate performance of different cooling pad material. Int J Sci Res Dev 2016;4:21–7.

[79] De Melo JCF, Bamberg JVM, MacHado NS, Caldas ENG, Rodrigues MS. Evaporative cooling efficiency of pads consisting of vegetable loofah. Comun Sci 2019;10:38–44. https://doi.org/10.14295/cs.v10i1.2930.

[80] Soponpongpipat N, Kositchaimongkol S. Recycled High-Density polyethylene and rice husk as a wetted pad in evaporative cooling system. Am J Appl Sci 2011;8:186–91. https://doi.org/10.3844/ajassp.2011.186.191.

[81] Niyomvas B, Potakarat B. Performance study of cooling pads. Adv Mater Res 2013;664:931–5. https://dx.doi.org/10.4028/www.scientific.net/AMR.664.931.

[82] Pandelidis D, Pacak A, Cicho A, Gizicki W, Worek W, Cetin S. Experimental study of plate materials for evaporative air coolers. Int Commun Heat Mass Tran 2020. https://doi.org/10.1016/j.icheatmasstransfer.2020.105049.

[83] Velasco-Gómez E, Tejero-González A, Jorge-Rico J, Rey-Martínez FJ. Experimental investigation of the potential of a new fabric-based evaporative cooling pad. Sustain Times 2020;12. https://doi.org/10.3390/su12177070.

[84] Martínez P, Ruiz J, Martínez PJ, Kaiser AS, Lucas M. Experimental study of the energy and exergy performance of a plastic mesh evaporative pad used in air conditioning applications. Appl Therm Eng 2018;138:675–85. https://doi.org/10.1016/j.applthermaleng.2018.04.065.

[85] Chen X, Su Y, Aydin D, Zhang X, Ding Y, Reay D, et al. Experimental investigations of polymer hollow fibre integrated evaporative cooling system with the fibre bundles in a spindle shape. Energy Build 2017;154:166–74. https://doi.org/10.1016/j.enbuild.2017.08.068.

[86] Chen X, Su Y, Aydin D, Ding Y, Zhang S, Reay D, et al. A novel evaporative cooling system with a polymer hollow fibre spindle. Appl Therm Eng 2018;132:665–75. https://doi.org/10.1016/j.applthermaleng.2018.01.005.

[87] He J, Hoyano A. Experimental study of cooling effects of a passive evaporative cooling wall constructed of porous ceramics with high water soaking-up ability. Build Environ 2010;45:461–72. https://doi.org/10.1016/j.buildenv.2009.07.002.

[88] He J, Hoyano A. Experimental study of practical applications of a passive evaporative cooling wall with high water soaking-up ability. Build Environ 2011;46:98–108. https://doi.org/10.1016/j.buildenv.2010.07.004.

[89] Zeitoun O, Ali M, Al-Ansary H, Nuhait A. Ceramic tubes membrane technology as a new humidification technique for gas turbine inlet air cooling. Int J Therm Sci 2014;80:1–10. https://doi.org/10.1016/j.ijthermalsci.2014.01.019.

[90] Chen W, Liu S, Lin J. Analysis on the passive evaporative cooling wall constructed of porous ceramic pipes with water sucking ability. Energy Build 2015;86:541–9. https://doi.org/10.1016/j.enbuild.2014.10.055.

[91] Laknizi A, Ben Abdellah A, Faqir M, Essadiqi E, Dhimdi S. Performance characterization of a direct evaporative cooling pad based on pottery material. Int J Sustain Eng 2019:1–11. https://doi.org/10.1080/19397038.2019.1677800. 00.

[92] Ibrahim E, Shao L, Riffat SB. Performance of porous ceramic evaporators for building cooling application. Energy Build 2003;35:941–9. https://doi.org/10.1016/S0378-7788(03)00019-7.

[93] Sellami K, Feddaoui M, Labsi N, Najim M, Oubella M, Benkahla YK. Direct evaporative cooling performance of ambient air using a ceramic wet porous layer. Chem Eng Res Des 2019;142:225–36. https://doi.org/10.1016/j.cherd.2018.12.009.

[94] Abdullah A, Said I Bin, Ossen DR. A sustainable bio-inspired cooling unit for hot arid regions: integrated evaporative cooling system in wind tower. Appl Therm Eng 2019;161:114201. https://doi.org/10.1016/j.applthermaleng.2019.114201.
[95] Sudprasert S, Sankaewthong S. Utilization of rice husks in a water-permeable material for passive evaporative cooling. Case Stud Constr Mater 2018;8:51–60. https://doi.org/10.1016/j.cscm.2017.12.005.
[96] Korese JK, Hensel O. Experimental evaluation of bulk charcoal pad configuration on evaporative cooling effectiveness. Agric Eng Int CIGR J 2016;18:11–21.
[97] Tejero-González A, Andrés-Chicote M, García-Ibáñez P, Velasco-Gómez E, Rey-Martínez FJ. Assessing the applicability of passive cooling and heating techniques through climate factors: an overview. Renew Sustain Energy Rev 2016;65:727–42. https://doi.org/10.1016/j.rser.2016.06.077.
[98] Purswell JL, Linhoss JE, Edge CM, Davis JD, Campbell JC. Water supply rates for recirculating evaporative cooling systems. Appl Eng Agric ASABE 2018;34:581–90.
[99] Sellami K, Feddaoui M, Labsi N, Najim M, Benkahla YK. Numerical simulations of heat and mass transfer process of a direct evaporative cooler from a porous layer. J Heat Tran 2019;141:1–10. https://doi.org/10.1115/1.4043302.
[100] Gilani N, Poshtiri AH. Heat exchanger design of direct evaporative cooler based on outdoor and indoor environmental conditions. J Therm Sci Eng Appl 2014;6:1–9. https://doi.org/10.1115/1.4028179.